Article

Rapid Synthesis of Asymmetric Methyl-Alkyl Carbonates Catalyzed by α-KMgPO$_4$ in a Sealed-Vessel Reactor Monowave 50

Tiefeng Wang [1], Xu Li [1], Xiaosheng Zhang [1] and Jinxiang Dong [1,2,*]

[1] College of Chemistry and Chemical Engineering, Taiyuan University of Technology, Taiyuan 030024, China; wangtiefeng0072@link.tyut.edu.cn (T.W.); lixu0121@126.com (X.L.); zhxsh77@126.com (X.Z.)

[2] School of Chemical Engineering and Light Industry, Guangdong University of Technology, Guangzhou 510006, China

* Correspondence: dongjinxiang@tyut.edu.cn or dongjinxiangwork@hotmail.com; Tel.: +86-0351-6010-5508

Abstract: Dimethyl-carbonate (DMC) is a green carboxymethylation agent for synthesis of the versatile long-chain alkyl carbonates through base-catalyzed transesterification with aliphatic alcohols. Herein, we demonstrated the facile preparation of a novel heterogeneous base catalyst α-KMgPO$_4$ using commercially cheap metal salts via hydrothermal-calcination procedure. The combination of temperature programmed desorption (TPD) and FTIR measurements with CO$_2$ pre-adsorbed revealed the presence of weak and medium base sites on α-KMgPO$_4$. Furthermore, α-KMgPO$_4$ catalyzed transesterification of DMC and n-octanol was performed in a sealed-vessel reactor (Monowave 50). The results show that the reaction was completed in only 10 min with the 97.5% conversion of n-octanol and >99% selectivity to asymmetric methyl-octyl carbonate under the optimal conditions. Additionally, the possible catalytic mechanism is proposed. As an extended contribution, the tribology performance of the asymmetric methyl-alkyl carbonates was further evaluated.

Keywords: catalyst; α-KMgPO$_4$; transesterification; asymmetric carbonates; Monowave 50 reactor

1. Introduction

Di-alkyl carbonates have been recognized as an environmentally benign and valuable organic compounds which have increasing applications in many fields, such as organic synthesis, electronic industry, fuel additive, transportation, etc. [1–3]. In particular, with the popularity of lithium batteries and concern of green chemicals, di-alkyl carbonates aroused widespread attention due to their excellent performance, nontoxicity and biodegradability. The conventional synthesis methods for alkyl carbonates are harmful for health and highly toxic because of the use of phosgene, halo compounds or dimethyl sulfate [4], which are undesirable in green chemistry the perspective. Recently, alternative methodologies have been continuously developed to obtain asymmetrical alkyl carbonates (AACs); among them, the transesterification method is accepted gradually and promoted, which can be triggered by the lighter alkyl carbonates such as dimethyl carbonate (DMC) as the efficient carbonylating agent [5] for aliphatic alcohols. This route has better ecological compatibility by the employment of eco-friendly nonpetroleum monomer DMC [6], and the methanol co-product can be recyclable to synthesize DMC [7].

Various catalysts have been investigated for the DMC mediated carboxymethylation reactions. The first type was acid, either Lewis or Brønsted acid [8,9]. Then, there was an enzyme catalyst named Novozym 435 [10]. However, a long time was required to reach reaction equilibrium. In general, the basic catalyst represented by potassium carbonate [11,12] was the first considered catalyst, followed by others such as TBD (1,5,7-Triazabicyclo[4.4.0]dec-5-ene) [13–15], nano-crystalline MgO [16], MgLa mixed oxides [17], Lanthanum(III) isopropoxide [18], Bu$_2$SnMoO$_4$ [19] etc. However, some catalysts do not show enough activity, or face problems such as regeneration, causticity and high cost.

Therefore, to develop an innovative catalyst which is highly active, eco-friendly, low-cost and stable is desirable for this reaction and beneficial to expanding the potential range of carboxymethylation for DMC chemistry in fundamental research. Herein, a novel basic catalyst is introduced that has never been used, called α-KMgPO$_4$, which has a good basic site to provide high and reusable catalytic activity to efficiently synthesize two asymmetric carbonates of methyl-octyl carbonate (MOC) and methyl-lauryl carbonate (MLC). Simultaneously, it is cost-effective because of the use of cheap metal salts and easy to recycle. α-KMgPO$_4$ is emerging as a promising heterogeneous catalyst for this type of reaction.

At present, it should be noted that this carbonate interchange reaction is mostly conducted under reflux operation or in autoclave [20,21], which performed a slower reaction rate. As is known, the microwave-assisted method is conducive to accelerate the reaction rate. It is a tool for organic synthesis and sustainable chemistry [22], which is related to the purely thermal phenomena of microwaves according to the experimental evidence [23–25]. There is a reactor named Monowave 50 (Anton Paar GmbH) whose heating and cooling curves or reaction results can adequately mimic the modern microwave reactors [26]. In this work, Monowave 50 reactor was committed to the reaction equilibrium that could be established rapidly. The reaction conditions were investigated on this platform, the detailed reaction results analyzed and the possible reaction mechanisms postulated. The fluid compounds containing carbonate group have shown potential application value in the field of synthetic lubricants [27]. Therefore, the tribology performance of the synthesized carbonates was tested.

2. Results and Discussion

Figure 1a shows the X-ray powder patterns of α-KMgPO$_4$. According to the results in [28], α-KMgPO$_4$ was prepared successfully by our method.

Figure 1. (**a**) X-ray powder patterns of α-KMgPO$_4$; (**b**) FTIR spectrum of α-KMgPO$_4$; (**c**) SEM image of α-KMgPO$_4$; and (**d**) CO$_2$-TPD.

The FTIR spectrum of α-KMgPO$_4$ is shown in Figure 1b. The absorption bands in the range of 1120–1000 cm^{-1} should be assigned to the asymmetric stretching P-O vibrations of the phosphorus tetrahedral and the band at 960 cm^{-1} is the symmetric stretching vibration of P-O [29,30]. The bands at 500–650 and 460 cm^{-1} are due to asymmetric and symmetric

bending P-O vibration, respectively [30]. The bands at 496 cm^{-1} could be attributed to the stretching vibration of Mg-O [31].

　　SEM micrograph of α-KMgPO$_4$ is shown in Figure 1c. Stunningly, the material was in the shape of a beautiful flower cluster under our lens. The resulting particles ranged in size from 30 to 40 μm.

　　The surface base properties of α-KMgPO$_4$ were investigated by the combination of TPD and FTIR measurements with CO$_2$ pre-adsorbed. For CO$_2$-TPD, the CO$_2$ desorption curve was recorded (Figure 1d). A wide peak was shown over the entire temperature range. The desorption curve could be deconvoluted into two main peaks approximately before 400 °C. According to the authors of [32,33], the first peak at about 140 °C represents sites with weak basicity, and the peak at 280 °C shows sites with medium basicity, revealing the coexistence of weak and medium strength basic sites [32]. It was also obvious that the medium strength base takes a dominant share. The detail of the basicity is listed in Table 1.

Table 1. The detail of basicity.

Peak	Temperature (°C)	Basicity Type	Peak Area Ratio	Relative Basic Sites (mmolgcat^{-1})
1st	140	Weak	0.31	0.015
2nd	280	Medium	0.69	0.033

　　As shown in Figure 2, CO$_2$ was desorbed as temperature increases and various forms of CO$_2$ adsorption species were present: unidentate carbonate (U.C.) and bidentate carbonate (B.C.) could coexist because there were two coordinations of Mg-O in the material [28]. One was that Mg-O (5) was capable of producing bidentate carbonate, which shows a symmetric O-C-O stretching at 1340–1360 cm^{-1} and an asymmetric O-C-O stretching at 1610–1650 cm^{-1}. The other was Mg-O (4), which forms unidentate carbonate and exhibits a symmetric O-C-O stretching at 1380–1410 cm^{-1} and an asymmetric O-C-O stretching at 1510–1550 cm^{-1} [34,35]. The bands representing U.C. and B.C. were weak and basically disappeared at 200 °C, which could correspond to the first peak in CO$_2$-TPD. In addition, the four absorption bands (1921, 1974, 2045 and 2106 cm^{-1}) were unclear, which may be due to the presence of PO$_4$ tetrahedral [36] that enhances the basicity of the material. It can be seen that these absorption bands disappear at 300 °C, which is shown as the second peak representing the medium base in CO$_2$-TPD.

　　The catalytic performance was investigated by the synthesis of MOC. The conversion and selectivity were calculated based on n-octanol and MOC, respectively.

　　Five temperatures were adopted to illustrate the effect with an interval of 20 °C (Figure 3a). Only a very small amount of n-octanol was converted at 120 °C. With the temperature increase, conversion rises dramatically, up to 95.7% at 160 °C. The conversion elevated slightly and kept stabilized when >160 °C, reaching 97.2% at 180 °C. The selectivity showed a slight decline because a trace amount of di-octyl ether was co-produced with the increase of temperature. Therefore, 180 °C can be considered as the optimum temperature.

　　As shown in Figure 3b, an excellent conversion and selectivity were embodied at the molar ratio of 3.5:1, and there was a minor change when the ratio increased. From 3.5:1 to 14:1, the trend of conversion gradually increased due to the shift of the reaction equilibrium toward the product direction. With a further increase in the molar ratio, a slight decrease appeared at 17:1, which is likely related to the amount of DMC that played a role as diluting solvent. At the same time, the selectivity increased, indicating the side reaction of di-octyl ether was suppressed.
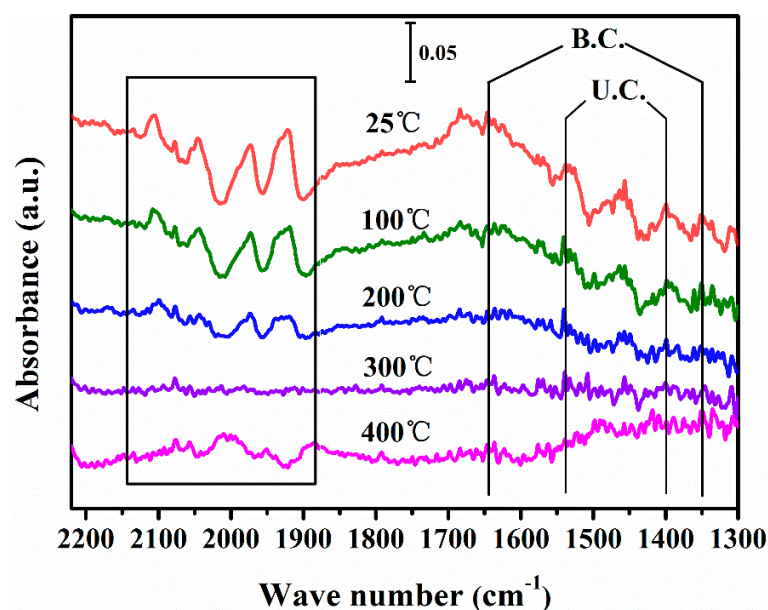
Figure 2. FTIR spectra of CO_2 adsorbed at room temperature on α-$KMgPO_4$ and desorbed at increasing evacuation temperatures.
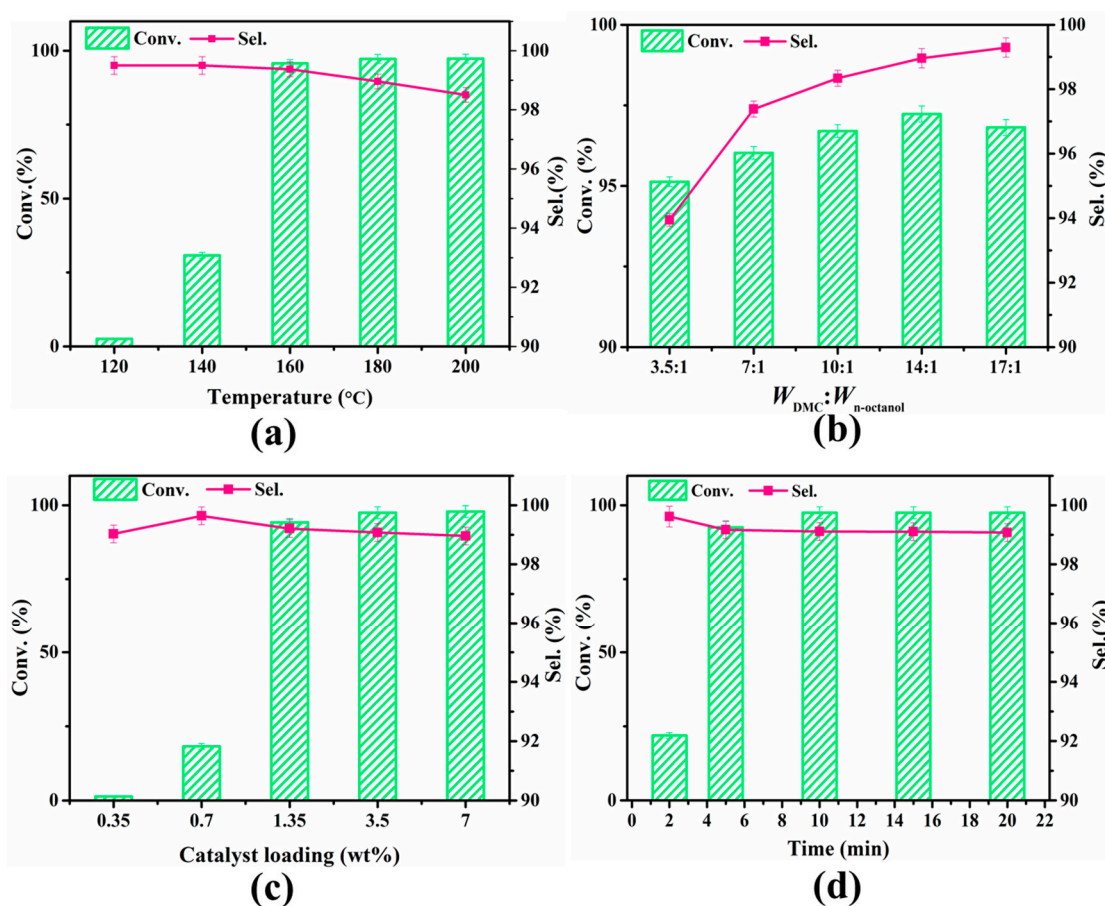

Figure 3. (**a**) Effect of reaction temperature; (**b**) effect of mass feed ratio of DMC: n-octanol; (**c**) effect of catalyst loading; and (**d**) effect of reaction time.

The amount of catalyst shows a prominent effect on reaction results (Figure 3c). An increasing conversion was observed with the catalyst loading (mass fraction of liquid) from

0.35 to 3.5 wt.%, and then it almost remained unchanged at 3.5 and 7 wt.%. At the loading of 3.5 wt.%, when other conditions were fixed, the conversion was 97.5% and the selectivity was maintained at ~99%. The excellent activity and chemical selectivity of the catalyst was proven.

The reaction time was also investigated in the case of the Monowave 50 reactor used. The conversion could reach 92.5% after 5 min, and the reaction was basically completed when the time was extended to 10 min with conversion improving to 97.5%. The selectivity was still held at >99% in the operated time range (Figure 3d). Compared with the reaction promoted by classic potassium carbonate in stainless steel autoclave, the reaction time was shortened from 2.5 h [20] to only a few minutes, which was inseparable from the application of the microwave-like heating curve.

For the reusability experiments, the synthesis of MOC was run for five consecutive cycles under the same conditions (Figure 4). All five cycles show a high conversion (~97.5%) and selectivity (~99%), without obvious catalyst deactivation after five cycles, which proves that the catalyst has stable catalytic activity. Figure 5a,b shows the XRD pattern and FTIR absorption spectrum of the catalyst before and after five reaction cycles. It revealed that there was no significant structural change of α-KMgPO$_4$ after reaction. Figure 5c shows the catalyst was broken and appeared fragmentation, which is due to the mechanical stirring. The data comparison showed that the catalyst could maintain its high activity and structure feature after five cycles, further highlighting its stability.
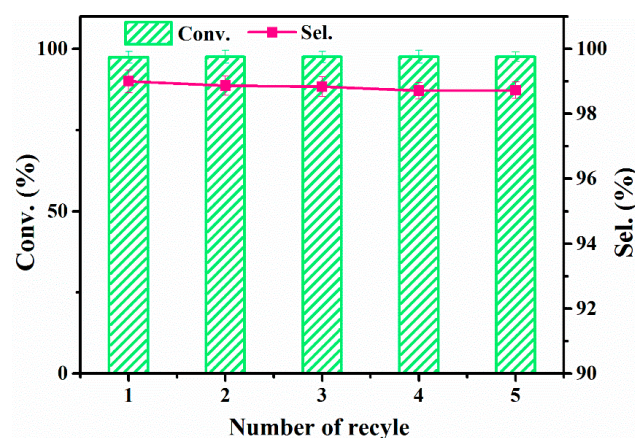

Figure 4. Reusability test (180 °C, W_{DMC}:$W_{\text{n-octanol}}$= 14:1, $w_{\text{cat.}}$ = 3.5 wt.%, 10 min).
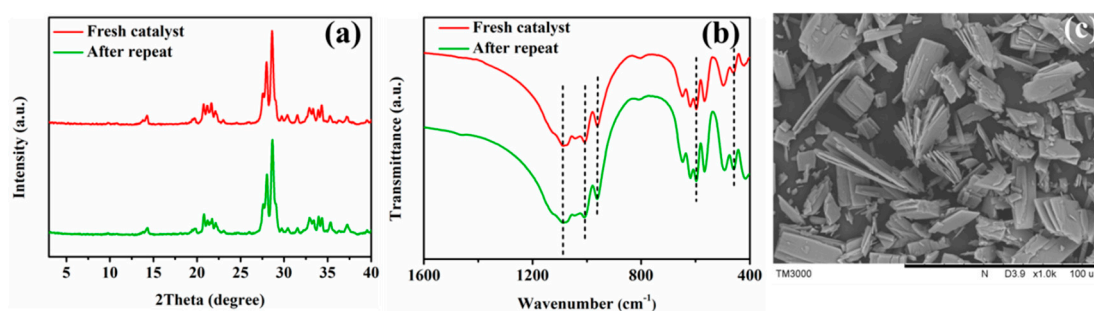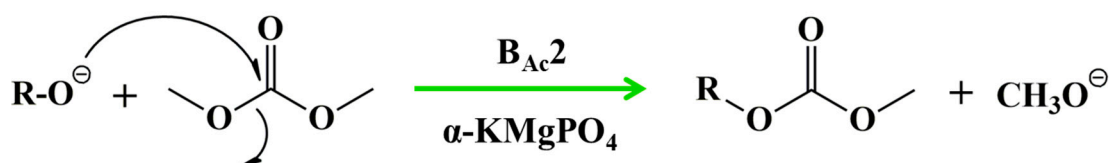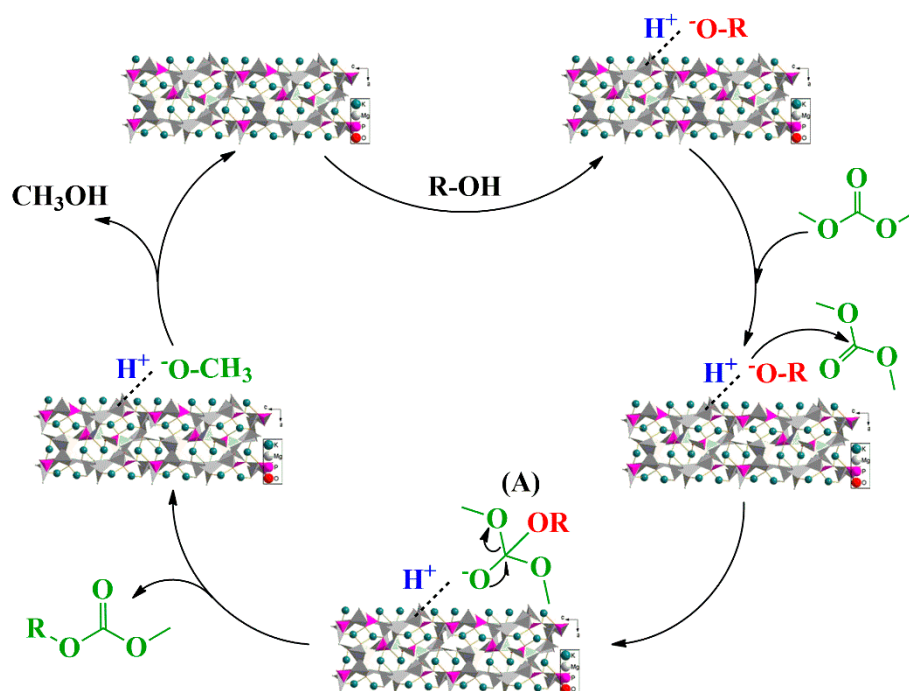

Figure 5. (**a**) PXRD; (**b**) FTIR; and (**c**) SEM of catalyst after five cycles.

The alkyl alcohol was carboxymethylated according to the B$_{\mathrm{Ac}}$2 mechanism [37] in the presence of α-KMgPO$_4$ (Scheme 1). Based on this process, the proposed reaction mechanism is shown in Scheme 2. The catalytic cycle begins with the adsorption of R-OH on the catalyst and the formation of RO$^-$ due to the presence of basic site. RO$^-$ can attack the carbonyl carbon atom of DMC, which was also adsorbed on the catalyst and further formed the tetrahedral intermediate (A). Under the impetus of O$^-$, CH$_3$O$^-$ is eliminated

to generate the corresponding carbonate, which is then desorbed from the catalyst. Finally, the catalytic cycle was completed by releasing CH_3OH.

Scheme 1. Synthesis scheme of ROCOOCH$_3$ from alkyl alcohol (R = octyl, laurel).
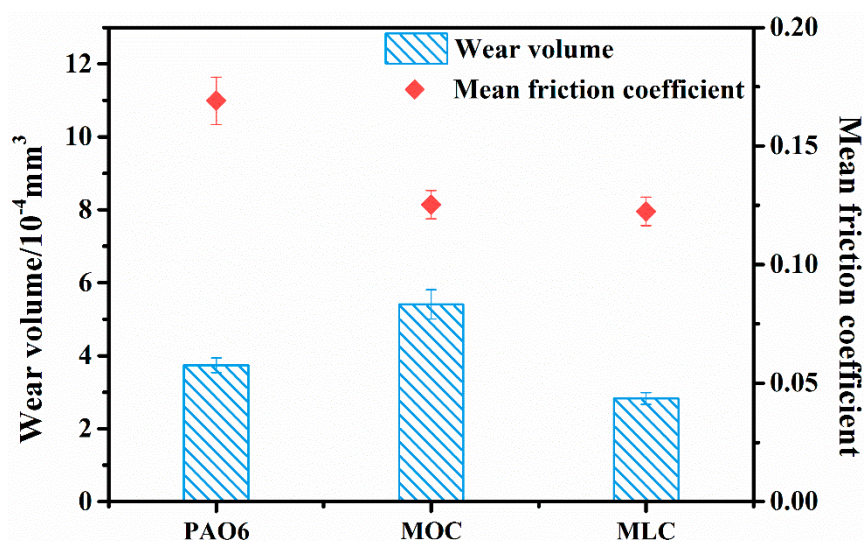

Scheme 2. Proposed reaction mechanism for the transesterification of alkyl alcohol with DMC.
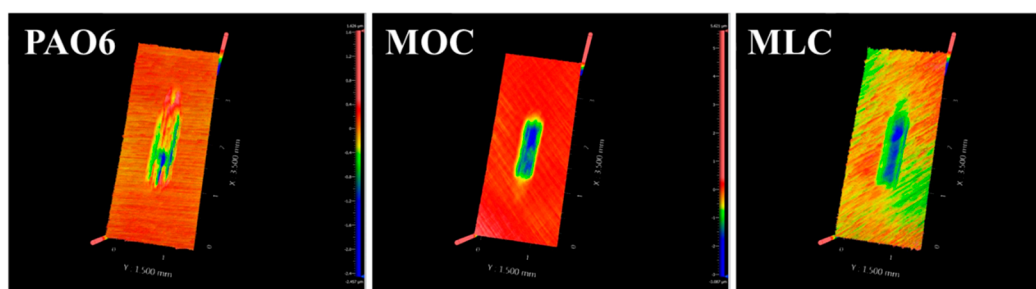
The analytical results by GC (see Figure S1) reveal the distribution of product; there are three peaks in the liquid product in the synthesis reaction of both MOC and MLC. Mass spectral analysis (Figure S2 and Table S1) allowed the peaks to be assigned to alkyl-alcohol, asymmetric carbonate and di-alkyl ether, respectively. The target product occupied an absolute share, while the residue alcohol and corresponding di-alkyl ethers were traces. The ^{13}C and ^{1}H NMR spectra are shown in Figure S3. Chemical shifts of the signal of residual ^{1}H in CDCl$_3$ occurred at 7.26 ppm and in ^{13}C signal at 77.0 ppm.

The friction and wear behaviors were evaluated under 100 N conditions by SRV-V tester. Figure 6a shows a comparison of the mean friction coefficient and wear volume of MOC, MLC and PAO 6. PAO 6 shows a friction coefficient of 0.169, which is greater than the others. For the two carbonates, approximately the same results were obtained. This can be attributed to the presence of characteristic group -OCOO-. Specifically, the strong polarity of the group reflects the adherence behavior on the surface of the friction pair [38], which affects the strength of the lubricant film. The friction-reducing performance of PAO 6 was worst because it has no polar groups. From the wear volume of lower disk, MLC shows the lowest value, better than that of PAO 6, which is due to the presence of carbonate molecules between metallic contacts that play a surfactant role [39]. The longer carbon chain (MLC) has a smaller wear volume than that of MOC, which reveals the effect of alkyl chain length on anti-wear; the length of the alkyl chain affects the thickness of the lubricating oil film to a certain extent. The lubricant film thickness was increased with the lengthening, resulting in the wear volume decreasing. 3D microscopic images of the wear

scars on the steel discs are provided in Figure 6b. The narrow and shallow wear track of MLC was more intuitive.

(a)

(b)

Figure 6. (**a**) The wear volume and mean friction coefficient; and (**b**) 3D microscopic images of wear tracks on the lower disks (SRV test, load 100 N, frequency 30 Hz, temperature 50 °C, duration 1 h).

The load-bearing capacity was tested by increasing the applied load from 150 N. As shown in Figure 7, when the load increased from 150 to 500 N, the mean friction coefficient of MOC and MLC decreased but wear volume increased. Furthermore, the seizure of two surfaces occurred when MOC was run at 600 N, and the wear volume was increased sharply. MLC operated relatively steadily until to 700 N MLC failed to withstand higher loads. Asymmetric alkyl carbonates exhibited excellent load bearing capacity, especially the longer is the alkyl chain, the higher is the critical load.
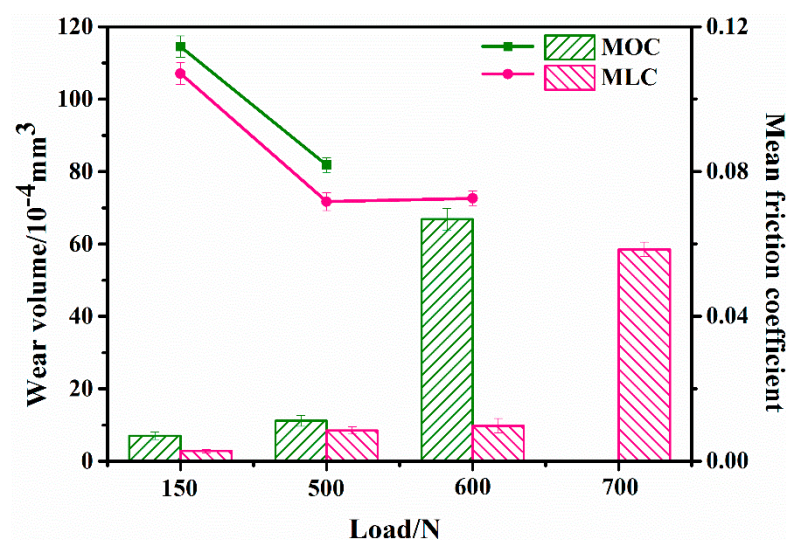
Figure 7. The wear volume (columns) and the mean friction coefficient (lines) for different applied loads for MOC and MLC (SRV test, frequency 30 Hz, temperature 50 °C, duration 1 h).

3. Experimental Section

3.1. Chemicals and Materials

Dimethyl carbonate (DMC, >98%), n-octanol (99.5%), lauryl alcohol (>98%), ethyl acetate (99%, AR), potassium phosphate dibasic anhydrous (K_2HPO_4, 99%) and magnesium chloride hexahydrate ($MgCl_2·6H_2O$) were purchased from Aladdin Industrial Corporation, Shanghai, China. Polyalpha-olefin (PAO 6) was purchased from Dowpol Chemical International Corp (Shanghai, China). All reagents were used without further treatment unless otherwise stated.

3.2. Catalyst Preparation and Characterization

The desired catalyst precursor was synthesized easily by the hydrothermal method [40]. The appropriate amounts of $MgCl_2·6H_2O$, K_2HPO_4 and deionized water were mixed together under stirring in a Teflon-lined autoclave. Then, the mixture was reacted at 180 °C for 24 h. Upon cooling to room temperature, the resulting precipitate was collected by filtration and washing with deionized water three times followed by drying. This precursor was weight (6.356 g) in a crucible and then heated at a ramp rate of 10 °C·min^{-1} up to 400 °C. The temperature was kept constant for 4 h in a Muffle furnace with air atmosphere. The resulting white powder was the activated catalyst α-KMgPO$_4$ (5.665 g) [28].

Powder X-ray diffraction (PXRD) was collected at room temperature on a diffractometer (Rigaku, MiniFlex II, Tokyo, Japan) with Cu Kα radiation (λ = 1.5418 Å). The measurements were recorded over a 2θ range of 3–40°. The synthesized catalyst was studied by Fourier-transform infrared absorption spectrum (Shimadzu IRAfnity−1 FTIR spectrometer, Japan) using the method of KBr tableting. The morphology and size of catalyst were identified by scanning electron microscopy (SEM, Hitachi, SU 8010, Tokyo, Japan). The base properties of α-KMgPO$_4$ were measured by temperature programmed desorption (TPD) and infrared spectroscopy of CO_2. For the CO_2-TPD experiment, the Quantachrome Instruments ChemBET (Boynton Beach, FL, USA) with a thermal conductivity detector (TCD) was used. First, 50 mg of catalyst were pretreated in situ at 300 °C under He flow (60 mL·min^{-1}) for 2 h and cooled down to 40 °C. Then, a flowing mixture of 5% of CO_2 in He (60 mL·min^{-1}) was adsorbed for 3 h. Weakly adsorbed CO_2 was removed by a He purge (20 mL·min^{-1}) for 1 h. Then, the desorption process was run in the He flow (20 mL·min^{-1}) by temperature increasing to 800 °C at a heating rate of 10 °C·min^{-1}. The evolved CO_2 was monitored by TCD. The FTIR analysis of CO_2 adsorbed was carried out on FTIR spectrometer (PerkinElmer, Frontier, Waltham, MA, USA) after CO_2 adsorption at room temperature (a flowing mixture of 10% CO_2 in He, 100 mL·min^{-1}, 2 h). Before the

adsorption process, a catalyst spectrum was taken. With the CO_2 evacuated at 25, 100, 200, 300 and 400 °C, the CO_2 adsorption spectra were recorded, and the spectra of the adsorbed species were obtained by subtracting the catalyst spectrum.

3.3. Catalyst Test

MOC was prepared by a mixture of n-octanol (0.325 g), DMC and the activated catalyst. These reactants were heated in a 10 mL seamless pressure vial (a sealed Pyrex microwave vessel) via a stainless steel heating jacket that allows a rapid heating and cooling to target temperature accurately. The reaction temperature and time were set by the operation panel, the "as fast as possible" mode (AFAP) was selected and the speed of magnetic stirring was fixed at 1000 r·min^{-1}. After the reaction was terminated, along with rapidly cooling down to 50 °C, the temperature and pressure curves were recorded (Figure S4). The catalyst was recovered by centrifugation and washing with ethyl acetate three times, and then it was dried at 80 °C. The upper liquid was collected and treated using a Rotavapor rotary evaporator (IKA RV 10 basic) at 50 °C to obtain the liquid product. MLC was synthesized in a similar process.

Reusability experiments were carried out after exploring the experimental condition. Under the optimal conditions, the first cycle was run, and then the upper liquid was processed and analyzed. The reacted catalyst was subjected to a next cycle without any treatment. For these experiments, the catalyst was used for five consecutive batch reactions. The final catalyst was recovered by the procedure described above.

The liquid product was monitored by gas chromatography (GC-2014 C, Shimadzu, Kyoto, Japan) equipped with an automatic column injector (330 °C), an FID detector (330 °C) and an Rxi-5 HT capillary column (30 m, 0.25 mm i.d., 0.25 μm film thickness, Restek). The column temperature was initially 50 °C for 2 min, gradually increased to 330 °C at 10 °C·min^{-1} and maintained at this level for 3 min. The conversion and selectivity were determined by gas chromatographic analyses. Gas chromatography–mass spectrometry (GCMS-QP 2010 Plus, Shimadzu, Japan) was operated with a Shimadzu GCMSQP 2010 Ultra mass spectrometer as detector, electrospray ionization (EI) (70 eV) and an Rxi-5 MS capillary column (30 m, 0.25 mm i.d., 0.25 μm film thickness, Restek). The full scan analysis was performed between m/z 20 and 400. The injector temperature was 290 °C and the capillary direct interface temperature was 290 °C. The carrier gas was helium at a flow rate of 1 mL·min^{-1}. The column temperature was initially 50 °C for 2 min, then gradually increased to 300 °C at 10 °C·min^{-1} and finally kept at 300 °C for 5 min. NMR spectra were recorded on a Bruker Advance III spectrometer at 400 MHz and $CDCl_3$ was used as solvent.

3.4. Tribology Test

The tribology behavior of asymmetric carbonates was evaluated from two aspects with an Optimol SRV-V oscillating reciprocating friction and wear tester. First, for the friction-reducing and anti-wear performance in a fixed load (100 N), pure poly-alpha-olefin (PAO) 6 was chosen for comparison under the same test conditions. Second, the carrying capacity at higher load was tested. The specific details of the steel plate and steel ball used are shown in the Supplementary Materials. The friction curves were recorded automatically with a computer interfaced to the SRV tester, and the corresponding mean friction coefficient was obtained. A 3D non-contact optical surface profiler (Zygo, Zegage, Middlefield, CT, USA) was used to record the images of representative wear scars and measure the wear volume of the lower disk.

4. Conclusions

We prepared a new basic catalyst α-$KMgPO_4$ to catalyze the transesterification reaction of alkyl alcohols with DMC. The basic properties of α-$KMgPO_4$ were characterized by the combination of TPD and FTIR measurements with CO_2 pre-adsorbed, revealing that the weak and medium bases exist simultaneously. The catalytic activity and stability

were proven by catalyzing the carboxymethylation reaction of n-octanol in Monowave 50 reactor. The reaction was completed in 10 min with 97.5% conversion of n-octanol and >99% selectivity to asymmetric methyl-octyl carbonate. The possible reaction mechanism relying on the basicity of the catalyst is proposed. Furthermore, the tribology test of AACs was performed, which showed superior friction-reducing and anti-wear ability and high load carrying capacity. Overall, this work covers the process from synthesis to application, with attractive sustainability features.

Supplementary Materials: The following are available online at https://www.mdpi.com/article/10.3390/catal11040499/s1, Figure S1: GC trace of the products: (a) MOC as the main product; (b) MLC as the main product, Figure S2: GC-MS spectrum of the liquid products, Table S1: Mass spectral data of MOC and MLC, Figure S3: NMR Data of MOC and MLC, Figure S4: The parameters recorded on Monowave 50 reactor; The specific details of the steel plate and steel ball used.

Author Contributions: Conceived and designed the experiments, T.W., X.L. and J.D.; provided the synthesis method of catalyst precursor, X.Z.; writing—original draft preparation, T.W.; writing—review and editing, X.L. and J.D. All authors have read and agreed to the published version of the manuscript.

Data Availability Statement: The data are contained within the article or the Supplementary Materials.

Conflicts of Interest: The authors declare no competing interests.

References

1. Chen, S.C.; Wang, H.; Kang, Z.X.; Jin, S.; Zhang, X.D.; Zheng, X.S.; Qi, Z.M.; Zhu, J.F.; Pan, B.C.; Xie, Y. Oxygen vacancy associated single-electron transfer for photofixation of CO_2 to long-chain chemicals. *Nat. Commun.* **2019**, *10*, 788–795. [CrossRef]
2. Huang, S.Y.; Yan, B.; Wang, S.P.; Ma, X.B. Recent advances in dialkyl carbonates synthesis and applications. *Chem. Soc. Rev.* **2015**, *44*, 3079–3116. [CrossRef]
3. Cattelan, L.; Fiorani, G.; Perosa, A.; Maschmeyer, T.; Selva, M. Two-Step Synthesis of Dialkyl Carbonates through Transcarbonation and Disproportionation Reactions Catalyzed by Calcined Hydrotalcites. *ACS Sustain. Chem. Eng.* **2018**, *6*, 9488–9497. [CrossRef]
4. Ramesh, S.; Devred, F.; Debecker, D.P. $NaAlO_2$ supported on titanium dioxide as solid base catalyst for the carboxymethylation of allyl alcohol with DMC. *Appl. Catal. A Gen.* **2019**, *581*, 31–36. [CrossRef]
5. Chen, Y.D.; Yang, Y.; Tian, S.L.; Ye, Z.B.; Tang, Q.; Ye, L.; Li, G. Highly effective synthesis of dimethyl carbonate over CuNi alloy nanoparticles @Porous organic polymers composite. *Appl. Catal. A Gen.* **2019**, *587*, 117275. [CrossRef]
6. Yang, Z.F.; Liu, L.; An, H.Z.; Li, C.H.; Zhang, Z.C.; Fang, W.J.; Xu, F.; Zhang, S.J. Cost-Effective Synthesis of High Molecular Weight Biobased Polycarbonate via Melt Polymerization of Isosorbide and Dimethyl Carbonate. *ACS Sustain. Chem. Eng.* **2020**, *8*, 9968–9979. [CrossRef]
7. Selva, M.; Perosa, A.; Rodríguez-Padrón, D.; Luque, R. Applications of Dimethyl Carbonate for the Chemical Upgrading of Biosourced Platform Chemicals. *ACS Sustain. Chem. Eng.* **2019**, *7*, 6471–6479. [CrossRef]
8. Jin, S.; Hunt, A.J.; Clark, J.H.; McElroy, C.R. Acid-catalysed carboxymethylation, methylation and dehydration of alcohols and phenols with dimethyl carbonate under mild conditions. *Green Chem.* **2016**, *18*, 5839–5844. [CrossRef]
9. Chevella, D.; Macharla, A.K.; Banothu, R.; Gajula, K.S.; Amrutham, V.; Boosa, M.; Nama, N. Synthesis of non-symmetrical alkyl carbonates from alcohols and DMC over the nanocrystalline ZSM-5 zeolite. *Green Chem.* **2019**, *21*, 2938–2945. [CrossRef]
10. Zhou, Y.L.; Jin, Q.Y.; Gao, Z.Y.; Guo, H.T.; Zhang, H.B.; Zhou, X.H. Asymmetric organic carbonate synthesis catalyzed by an enzyme with dimethyl carbonate: A fruitful sustainable alliance. *RSC Adv.* **2014**, *4*, 7013–7018. [CrossRef]
11. Tundo, P.; Trotta, F.; Moraglio, G.; Ligorati, F. Continuous-Flow Processes under Gas-Liquid Phase-Transfer Catalysis (GL-PTC) Conditions: The Reaction of Dialkyl Carbonates with Phenols, Alcohols, and Mercaptans. *Ind. Eng. Chem. Res.* **1988**, *27*, 1565–1571. [CrossRef]
12. Tundo, P.; Rossi, L.; Loris, A. Dimethyl Carbonate as an Ambident Electrophile. *J. Org. Chem.* **2005**, *70*, 2219–2224. [CrossRef]
13. Carloni, S.; Vos, D.E.D.; Jacobs, P.A.; Maggi, R.; Sartori, G.; Sartorio, R. Catalytic Activity of MCM-41–TBD in the Selective Preparation of Carbamates and Unsymmetrical Alkyl Carbonates from Diethyl Carbonate. *J. Catal.* **2002**, *205*, 199–204. [CrossRef]
14. Mutlu, H.; Ruiz, J.; Solleder, S.C.; Meier, M.A.R. TBD catalysis with dimethyl carbonate: A fruitful and sustainable alliance. *Green Chem.* **2012**, *14*, 1728–1735. [CrossRef]
15. Wu, L.Q.; Tian, S.B. Immobilization of 1,5,7-Triazabicyclo[4.4.0]dec-5-ene on Magnetic γ-Fe_2O_3Nanoparticles: A Highly Recyclable and Efficient Nanocatalyst for the Synthesis of Organic Carbonates. *Eur. J. Inorg. Chem.* **2014**, *2014*, 2080–2087. [CrossRef]

16. Kantam, M.L.; Pal, U.; Sreedhar, B.; Choudary, B.M. An Efficient Synthesis of Organic Carbonates using Nanocrystalline Magnesium Oxide. *Adv. Synth. Catal.* **2007**, *349*, 1671–1675. [CrossRef]

17. Veldurthy, B.; Figueras, F. An efficient synthesis of organic carbonates: Atom economic protocol with a new catalytic system. *Chem. Commun.* **2004**, *6*, 734–735. [CrossRef] [PubMed]

18. Hatano, M.; Kamiya, S.; Moriyama, K.; Ishihara, K. Lanthanum(III) Isopropoxide Catalyzed Chemoselective Transesterification of Dimethyl Carbonate and Methyl Carbamates. *Org. Lett.* **2011**, *13*, 430–433. [CrossRef] [PubMed]

19. Song, J.L.; Zhang, B.B.; Wu, T.B.; Yang, G.Y.; Han, B.X. Organotin-oxomolybdate coordination polymer as catalyst for synthesis of unsymmetrical organic carbonates. *Green Chem.* **2011**, *13*, 922–927. [CrossRef]

20. Tundo, P.; Memoli, S.; Hérault, D.; Hill, K. Synthesis of methylethers by reaction of alcohols with dimethylcarbonate. *Green Chem.* **2004**, *6*, 609–612. [CrossRef]

21. Tabanelli, T.; Cailotto, S.; Strachan, J.; Masters, A.F.; Maschmeyer, T.; Perosa, A.; Cavani, F. Process systems for the carbonate interchange reactions of DMC and alcohols: Efficient synthesis of catechol carbonate. *Catal. Sci. Technol.* **2018**, *8*, 1971–1980. [CrossRef]

22. Leadbeater, N.E. *Microwave Heating as a Tool for Sustainable Chemistry*, 1st ed.; CRC Press: Boca Raton, FL, USA, 2010.

23. Kappe, C.O.; Pieber, B.; Dallinger, D. Microwave effects in organic synthesis: Myth or reality? *Angew. Chem. Int. Ed.* **2013**, *52*, 1088–1094. [CrossRef]

24. Baghbanzadeh, M.; Carbone, L.; Cozzoli, P.D.; Kappe, C.O. Microwave-assisted synthesis of colloidal inorganic nanocrystals. *Angew. Chem. Int. Ed.* **2011**, *50*, 11312–11359. [CrossRef]

25. Kappe, C.O. My Twenty Years in Microwave Chemistry: From Kitchen Ovens to Microwaves that aren't Microwaves. *Chem. Rec.* **2019**, *18*, 1–26. [CrossRef]

26. Obermayer, D.; Znidar, D.; Glotz, G.; Stadler, A.; Dallinger, D.; Kappe, C.O. Design and Performance Validation of a Conductively Heated Sealed-Vessel Reactor for Organic Synthesis. *J. Org. Chem.* **2016**, *81*, 11788–11801. [CrossRef]

27. Rudnick, L.R.; Zecchini, C. Dialkyl Carbonates. In *Synthetics, Mineral Oils, and Bio-Based Lubricants-Chemistry and Technology*; Rudnick, L.R., Ed.; CRC Press: Boca Raton, FL, USA, 2020; pp. 264–271.

28. Wallez, G.; Colbeau-Justin, C.; Mercier, T.L.; Quarton, M.; Robert, F. Crystal Chemistry and Polymorphism of Potassium–Magnesium Monophosphate. *J. Solid State Chem.* **1998**, *136*, 175–180. [CrossRef]

29. Livitska, O.V.; Strutynska, N.Y.; Zatovsky, I.V.; Slobodyanik, N.S. The double phosphates $M^IM^{II}PO_4$ (M^I- Na, K; M^{II}- Mg, Mn, Co, Ni, Zn)—Synthesis from chloride melts and characterization. *Cryst. Res. Technol.* **2015**, *50*, 626–632. [CrossRef]

30. Korchemkin, I.V.; Pet'kov, I.V.; Kurazhkovskaya, V.S.; Borovikova, E.Y. Synthesis of sodium nickel phosphate and its crystallographic, spectroscopic, and temperature-controlled X-ray diffraction study. *Russ. J. Inorg. Chem.* **2015**, *60*, 265–269. [CrossRef]

31. Huang, X.; Li, N.; Wang, J.F.; Liu, D.F.; Xu, J.; Zhang, Z.J.; Zhong, M.F. Single Nanoporous $MgHPO_4 \cdot 1.2H_2O$ for Daytime Radiative Cooling. *ACS Appl. Mater. Interfaces* **2020**, *12*, 2252–2258. [CrossRef] [PubMed]

32. Rosset, M.; Féris, L.A.; Perez-Lopez, O.W. Biogas dry reforming over Ni-M-Al (M = K, Na and Li) layered double hydroxide-derived catalysts. *Catal. Today* **2020**. [CrossRef]

33. Ding, Y.D.; Song, G.; Zhu, X.; Chen, R.; Liao, Q. Synthesizing MgO with a high specific surface for carbon dioxide adsorption. *RSC Adv.* **2015**, *5*, 30929–30935. [CrossRef]

34. Belelli, P.G.; Ferretti, C.A.; Apesteguía, C.R.; Ferullo, R.M.; Cosimo, J.I.D. Glycerolysis of methyl oleate on MgO: Experimental and theoretical study of the reaction selectivity. *J. Catal.* **2015**, *323*, 132–144. [CrossRef]

35. Lercher, J.A.; Colombier, C.; Noller, H. Acid-Base Properties of Alumina-Magnesia Mixed Oxides. Part 4.—Infrared study of adsorption of carbon dioxide. *J. Chem. Soc. Faraday Trans. 1* **1984**, *80*, 949–959. [CrossRef]

36. Curini, M.; Epifano, F.; Marcotullio, M.C.; Rosati, O.; Tsadjout, A. Potassium Exchanged Layered Zirconium Phosphate as Base Catalyst in Knoevenagel Condensation. *Synth. Commun.* **2002**, *32*, 355–362. [CrossRef]

37. Aricò, F.; Tundo, P. *Methylethers from Alcohols and Dimethyl Carbonate, Encyclopedia of Inorganic and Bioinorganic Chemistry*; John Wiley & Sons, Ltd.: Hoboken, NJ, USA, 2016; pp. 1–14.

38. Gryglewicz, S.; Oko, F.A.; Gryglewicz, G. Synthesis of Modern Synthetic Oils Based on Dialkyl Carbonates. *Ind. Eng. Chem. Res.* **2003**, *42*, 5007–5010. [CrossRef]

39. Mujtaba, M.A.; Masjuki, H.H.; Kalam, M.A.; Noor, F.; Farooq, M.; Ong, H.C.; Gul, M.; Soudagar, M.E.M.; Bashir, S.; Fattah, I.M.R.; et al. Effect of Additivized Biodiesel Blends on Diesel Engine Performance, Emission, Tribological Characteristics, and Lubricant Tribology. *Energies* **2020**, *13*, 3375. [CrossRef]

40. Zhang, X.; Niu, W.X.; Dai, Y.J.; Xu, H.; Dong, J.X. Rapid selection of environmentally friendly layered alkaline-earth metal phosphates as solid lubricants using crystallographic data. *Sci. Rep.* **2018**, *8*, 1–11. [CrossRef]